Fachtagung "Experimentelle Strömungsmechanik"
5.–7. September 2023, München

Analysis of Reynolds Number and Surface Roughness Sensitivity of Surface Pressure on curved Roofs of Biogas Storage Tanks in reduced-scale Wind Tunnel Tests

Christof Gromke[1], Oliver Lippert[1], Olivier Eiff[2], Rosemarie Wagner[3]
[1] Laboratory of Building and Environmental Aerodynamics, Institute for Hydromechanics, Karlsruhe Institute of Technology
[2] Experimental Fluid Mechanics, Institute for Hydromechanics, Karlsruhe Institute of Technology
[3] Building Technology, Institute for Building Design and Technology, Karlsruhe Institute of Technology

Key words: building aerodynamics, wind engineering, atmospheric boundary layer, dome roof, sand grain roughness, passive flow control

Abstract

Surface pressure measurements on hemisphere and quarter-calotte roofs of reduced-scale models of low-pressure biogas tanks were performed in an atmospheric-boundary-layer wind tunnel. Since the geometries consist of curved surfaces without sharp edges (hemisphere) or without pronounced sharp edges (quarter-calotte), the first focus was on the sensitivity of the surface pressure to the Reynolds number which in reduced-scale wind tunnel investigations is usually two to three orders of magnitude smaller than at full-scale. To this end, investigations were performed for Reynolds numbers $4 \cdot 10^4 < Re < 2.7 \cdot 10^5$, with Re based on the diameter of the bottom circular ring wall and the velocity of the undisturbed approach flow at rooftop. Secondly, in order to study the effect of wall roughness on the surface pressure, experiments with models with smooth and rough surface were performed, whereby the roughness was realized by clueing sand grains to the surface.
The pressure coefficients c_p were found to be independent of Reynolds number for the models with smooth surface for $Re \geq 1.2 \cdot 10^5$ and for the models with rough surface for $Re \geq 8 \cdot 10^4$. The c_p-distributions on the hemisphere and quarter-calotte roof with smooth surface reflected a supercritical flow regime, while on the roofs with a rough surface they reflected a transcritical flow regime. The results indicate that pressure data obtained at reduced-scale models of low-pressure biogas tanks in atmospheric-boundary-layer wind tunnels can be reliably transferred to full-scale conditions where the supercritical or transcritical flow regime typically prevails.

Introduction

Biogas is a renewable energy source with utilization in the electricity, heat, and transport sector. A common means of storage are low-pressure biogas tanks with internal pressure less than 2-5 mbar, consisting of a bottom circular ring wall and a membrane covering. Typical geometries of the covering are hemispheres, calottes, or cones. The membrane covering is relatively flexible and vulnerable to wind loading. Damages after just a few years upon construction are not unusual and indicate the need for a better understanding of wind loading on such structures.

GALA e.V., Karlsruhe, Germany, ISBN 978-3-9816764-9-5

Reduced-scale wind tunnel studies on objects resembling low-pressure biogas tanks were performed on hemispheres or domes in the past. To the best of the authors' knowledge, the first studies on surface pressure distribution on dome-shaped roofs go back to Maher (1965) and Maher (1966). These studies, however, were not performed in an atmospheric-boundary-layer wind tunnel but in a standard aerodynamic wind tunnel with a relatively smooth floor and low turbulence intensity whereby the largest part of the scaled models (> 80%) was protruding out of the boundary layer. Surface-mounted hemispheres fully immersed in turbulent boundary layers were examined by Toy et al. (1983) and Savory and Toy (1986). They analyzed the effect of various approach flow characteristics (boundary-layer depth, turbulence intensity, Reynolds number) in combination with surface roughness (smooth, rough) on the surface pressure distribution. They found that for a low turbulence intensity approach flow (I_U < 4%), a rough hemisphere is necessary to obtain a Reynolds number independent surface pressure in reduced-scale experiments. Taylor (1991) investigated a hemisphere placed on a circular bottom ring in high turbulence intensity (15% < I_U < 25%) boundary layer flows. Although the hemisphere surface was smooth, a Reynolds number independent surface pressure distribution could be achieved in the reduced-scale experiments and was attributed to the relatively high turbulence intensity. The wind tunnel measurements of Cheng (2009) with smooth hemispheres found a minimum Reynolds number of $3 \cdot 10^5$ to obtain Re independent c_p-values for smooth and uniform approach flow, while for a turbulent boundary layer approach flow $Re_{min} = 1 \cdot 10^5$ was sufficient.
The above mentioned studies revealed basic parameters and boundary-layer conditions relevant for a reliable investigation of surface pressure on curved geometries in reduced-scale wind tunnel experiments. However, the actual approach flow characteristics and typical geometries of low-pressure biogas tanks were only approximately reached and none of the studies complied with all conditions at the same time. In particular, low-pressure biogas tanks are subjected to atmospheric-boundary-layer flows with higher turbulence intensities (typically 20% < I_U < 40%) and have hemisphere, calotte, or cone roofs mounted on the cylindrical wall of the fermenter. The present study aims to overcome these limitations in that it employs models with hemisphere and quarter-calotte roof on a bottom circular ring wall subjected to a boundary layer flow with turbulence intensities at the level of atmospheric flows.

Material and Methods

Reduced-scale models (M = 1:100) of low-pressure biogas tanks consisting of the cylindrical wall of the fermenter and a hemisphere or a quarter-calotte roof with height to diameter ratio of common biogas storage systems (Fig. 1) were studied in an atmospheric-boundary-layer wind tunnel. The models were realized with 'smooth' and 'rough' surface were made whereby in the latter case sand grains with diameter 0.75 < d_{sg} < 1.20 mm were clued to the surface (Lippert, 2023). The sand grains were randomly distributed on the ring wall and roof surfaces with an approximate average packing density of 0.08 grains/mm^2.

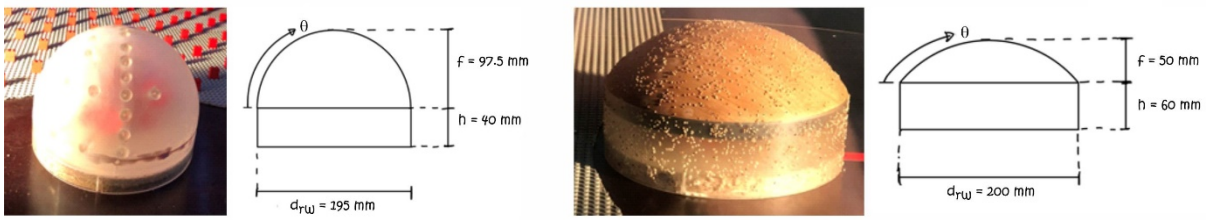

Fig. 1: Models of biogas tank with a 'smooth' hemisphere roof (left) and a 'rough' quarter-calotte roof (right), including model dimensions and altitude angle θ.

GALA e.V., Karlsruhe, Germany, ISBN 978-3-9816764-9-5

The models were subjected to a simulated atmospheric-boundary-layer approach flow with power law profile exponents $\alpha_U = 0.26$ for the streamwise mean velocity U(z) and $\alpha_I = -0.19$ for the streamwise turbulence intensity $I_U(z)$ according to

$$\frac{U(z)}{U_\delta} = \left(\frac{z}{z_\delta}\right)^{\alpha_U} \tag{1}$$

and

$$\frac{I_U(z)}{I_{U,\delta}} = \left(\frac{z}{z_\delta}\right)^{\alpha_I} \tag{2}$$

with z the height above ground, z_δ the boundary layer height, and U_δ and $I_{U,\delta}$ the mean freestream velocity and streamwise turbulence intensity at boundary layer height, respectively. The wind tunnel was operated at freestream velocities 5 m/s ≤ U_δ ≤ 33 m/s (Tab. 1). The turbulence intensity $I_U(z)$ decreased from ≈ 40% at the ground to 15 - 20% at the models' crest. Integral length scales $L_{u,x}$ estimated with Taylor's hypothesis of frozen turbulence, were found to be in the range between 200 and 400 mm for heights below the crests, i.e. approx. one to two bottom ring wall diameter d_{rw}. More details on the approach flow can be found in Frank and Ruck (2005), Ikhwan and Ruck (2006), or Gromke and Ruck (2008).
Time-resolved surface pressure measurements on the roofs of the biogas tanks were performed. The hemisphere and the quarter-calotte roofs were equipped with 62 taps at which pressures were simultaneously measured. Miniature pressure scanners (type ESP-32HD) in combination with a data acquisition system (type DTC Initium) were employed to record the pressures. Signals were sampled at a frequency $f_s = 1000$ Hz for a duration of 120 s. Assuming the advection velocity of the largest eddy structures ($L_{u,x}$) to be approximately the streamwise mean velocity U(z), the measurement duration of 120 s encompassed more than 1000 of their passages at $U_\delta = 5$ m/s and more than 7500 at $U_\delta = 33$ m/s, i.e. at least 1000 uncorrelated samples. The transfer function approach of Bergh and Tijdeman (1965) was applied to correct for frequency-dependent amplitude damping and phase shift distortions in the tubes connecting the measurement taps with the cavity of the pressure scanner.

Results

The surface pressure measurements were acquired at various freestream velocities U_δ, see Tab. 1. The measured pressure data p_{meas} were normalized by the dynamic pressure p_{dyn} which was calculated with the undisturbed approach flow velocity at crest height (U_{cr}) of the respective model to yield pressure coefficients c_p according to

$$c_p = \frac{p_{meas}}{p_{dyn}} = \frac{p_{meas}}{1/2\ \rho\ U_{cr}^2} \tag{3}$$

with ρ the density of air.
For the present study, the Reynolds number was based on the undisturbed approach flow velocity at crest height U_{cr} and the bottom ring wall diameter d_{rw} according to

$$Re = \frac{U_{cr}\ d_{rw}}{\nu} \tag{4}$$

with ν the kinematic viscosity of air.

GALA e.V., Karlsruhe, Germany, ISBN 978-3-9816764-9-5

An overview of the applied freestream velocities U_δ and the corresponding Reynolds numbers Re is provided in Tab. 1.

U_δ [m/s]		5	10	15	20	23	26	28	30	32	33
hemisphere	U_{cr}	3.2	6.3	9.5	12.7	14.6	16.4	17.7	19.0	20.2	20.9
(d_{rw} = 0.195 m)	Re_{hs}	4.1E4	8.2E4	1.2E5	1.6E5	1.9E5	2.1E5	2.3E5	2.5E5	2.6E5	2.7E5
1/4-calotte	U_{cr}	3.0	6.0	9.0	11.9	13.7	15.5	16.7	17.9	19.1	19.7
(d_{rw} = 0.2 m)	Re_{qc}	4.0E4	8.0E4	1.2E5	1.6E5	1.8E5	2.1E5	2.2E5	2.4E5	2.5E5	2.6E5

Tab. 1: Freestream velocities U_δ, velocity at crest height U_{cr}, Reynolds numbers Re; hs: hemisphere, qc: quarter-calotte.

Smooth hemisphere roof

Contour plots with the distribution of the mean pressure coefficient $c_{p,mean}$ according to Eq. (3) on the smooth hemisphere roof at selected Reynolds numbers Re (Eq. 4) are provided in Fig. 2. An intercomparison reveals the largest difference between the lowest and the highest Reynolds number. The variability with Re of the c_p-values is larger at the lowest Reynolds numbers and is stronger in the suction zone, in particular in the crest region. In the overpressure region, i.e. at low altitude angle θ, no pronounced variability can be identified even at the lowest Reynolds numbers. Overall, the distribution of pressure coefficients appears to be independent to Reynolds numbers for $Re \geq 1.2 \cdot 10^5$.

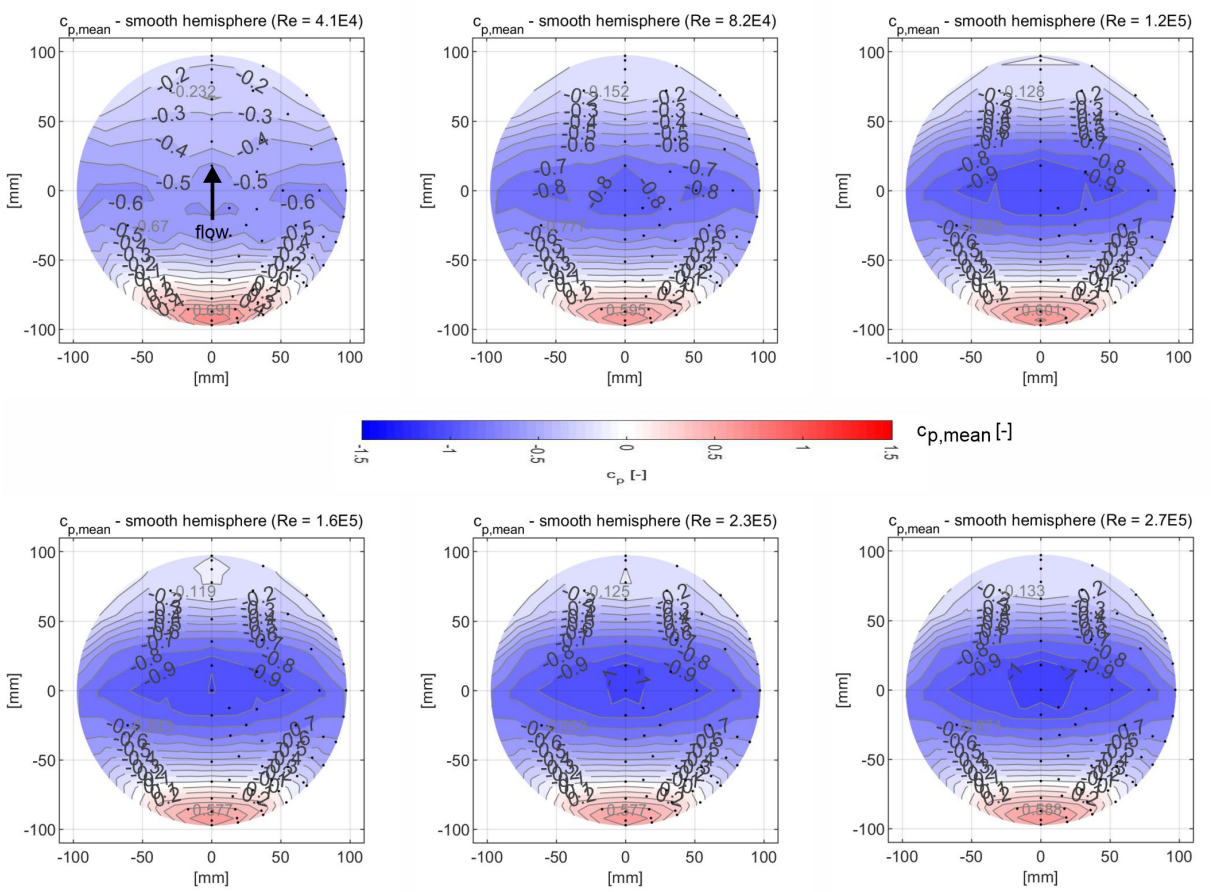

Fig. 2: Distribution of mean pressure coefficient $c_{p,mean}$ on the smooth hemisphere roof at selected Reynolds numbers Re. The black dots indicate the positions of the pressure measurement taps.

GALA e.V., Karlsruhe, Germany, ISBN 978-3-9816764-9-5

Since the $c_{p,mean}$-distribution has a distinct gradient in streamwise direction – except at the eave – the further analysis and discussion focusses on locations on the central streamwise arch line. Fig. 3a shows $c_{p,mean}$-values along the central streamwise arch line for all investigated Reynolds numbers (Tab. 1). At the two lowest Re, marked differences in comparison to the flows at higher Reynolds numbers occur with maximum absolute deviations in the crest region of $\Delta c_p \approx 0.5$ and 0.2, corresponding to relative deviations of approximately 50% and 20%. In the overpressure and base pressure region ($\theta > 140°$), distinct deviations can be seen only at the lowest Re with larger absolute c_p-values. In particular, in the base pressure region, the suction c_p-values at the lowest Re are approximately 150% larger than those of the higher Reynolds number flows.

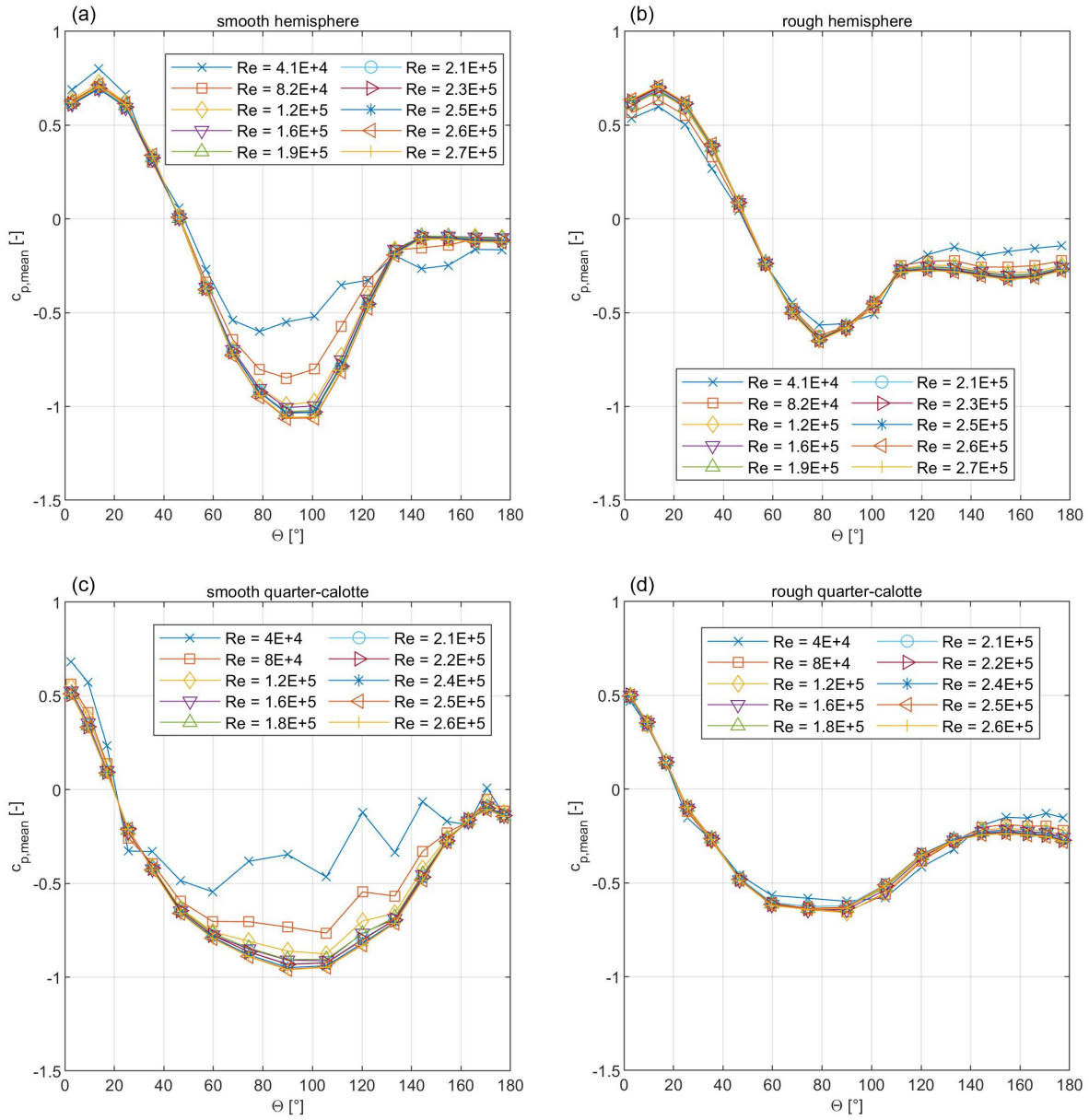

Fig. 3: Distribution of mean pressure coefficient $c_{p,mean}$ along the central streamwise arch line on smooth hemisphere roof (a), rough hemisphere roof (b), smooth quarter-calotte roof (c), and rough quarter-calotte roof (d).

GALA e.V., Karlsruhe, Germany, ISBN 978-3-9816764-9-5

Rough hemisphere roof

The $c_{p,mean}$-distribution along the central streamwise arch line on the rough hemisphere roof is shown in Fig. 3b. Only the pressure coefficients at the lowest Re show a clear deviation from those of the higher Reynolds number flows, hence, suggesting a Reynolds number independent surface pressure field for $Re \geq 8.2 \cdot 10^4$. Overall, at the rough hemisphere the variability among the various Reynolds numbers is smaller than at the smooth hemisphere (Fig. 3a). The c_p-distributions at high Reynolds show compared to those of the smooth hemisphere quantitative differences in the crest region with lower suction c_p-values and in the base pressure region with larger suction c_p-values. Moreover, on the rough hemisphere, the base pressure region is larger, beginning at $\theta \approx 110°$, hence indicating an earlier separation of the boundary layer from the surface.

Smooth quarter-calotte roof

The variability of the $c_{p,mean}$-distribution with Reynolds number on the smooth quarter-calotte roof is presented in Fig. 3c. As with the smooth hemisphere (Fig. 3a), notable differences exist only at the two lowest Re with the largest deviations in the crest region where the absolute suction c_p-values increase with increasing Re, and the surface pressure field achieves Reynolds number independence at $Re = 1.2 \cdot 10^5$. A comparison with the smooth hemisphere roof reveals slightly lower absolute c_p-values in the overpressure and in the crest region. Furthermore, in contrast to the hemisphere roof, a base pressure region with constant suction pressure cannot be identified, see also the contour plots provided in Fig. 4. The latter suggest an attached boundary layer over the entire smooth quarter-calotte roof.

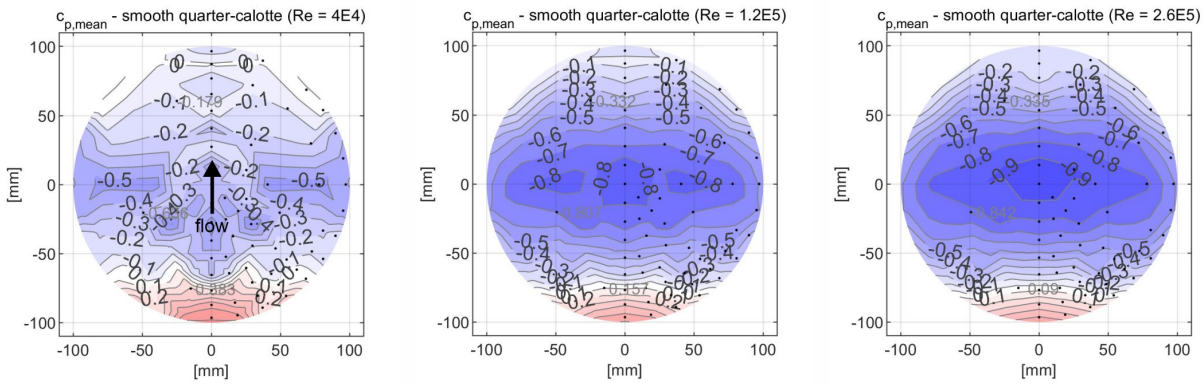

Fig. 4: Distribution of mean pressure coefficient $c_{p,mean}$ on the smooth quarter-calotte roof at selected Reynolds numbers Re (see Fig. 2 for color bar). The black dots indicate the positions of the pressure measurement taps.

Rough quarter-calotte roof

Fig. 3d present the $c_{p,mean}$-distribution along the central streamwise arch line on the rough quarter-calotte roof. Analogous to the rough hemisphere roof (Fig. 3b), noticeable deviations in the pressure coefficients can be found only at the lowest Re and, overall, the variability among the Reynolds numbers is smaller than at the smooth quarter-calotte roof. A Reynolds number independent surface pressure field is obtained at $Re = 8.0 \cdot 10^4$. In contrary to the

GALA e.V., Karlsruhe, Germany, ISBN 978-3-9816764-9-5

smooth quarter-calotte roof, a region with fairly constant base pressure appears, beginning at $\theta \approx 140°$, hence indicating boundary layer separation.

Discussion

The present atmospheric-boundary-layer wind tunnel study yielded Reynolds number independent mean pressure coefficients $c_{p,mean}$ on hemisphere and quarter-calotte roofs of low-pressure biogas tanks with smooth surface for $Re \geq 1.2 \cdot 10^5$ and with rough surface for $Re \geq 8 \cdot 10^4$. As such, these findings are in line with those of previous works on hemispheres and domes with regard to the effects of approach flow turbulence characteristics and surface roughness on Reynolds number independency (Toy et al., 1983; Savory and Toy, 1986;. Taylor, 1991; Cheng, 2009). However, an interesting aspect is whether the observed Reynolds number independent pressure distributions are representative of a subcritical, critical, supercritical, or transcritical flow regime, i.e. whether or not the drag crisis is still to occur with increasing Re. This is in particular relevant to the transferability of the obtained pressure data to full-scale conditions since at low-pressure biogas tanks the supercritical or transcritical regime prevail at moderate or high wind speeds.
Investigations with smooth sphere in uniform and low turbulence flows, e.g. Achenbach (1972), show the critical regime at $3 \cdot 10^5 < Re < 4 \cdot 10^5$. The ranges of the critical regime in the present experiments with the smooth and rough surfaces are presumably lower. This is because of the high turbulence intensity of the approach flow, its boundary layer profile, and the surface in the case of a rough roof. Moreover, in the case of the quarter-calotte, a non-continuously differentiable transition between the bottom ring wall and the roof exists at the eave, forming a 'semi-sharp' edge and is deemed to shift the critical flow regime to lower Reynolds numbers.
Based on the $c_{p,mean}$-distributions along the central streamwise arch line in Fig. 3, it is hypothesized that a supercritical flow regime is present in the case of the smooth surface and a transcritical flow regime in the case of a rough surface at both the hemisphere and quarter-calotte roof. Indirect evidence for this hypothesis is provided by high Reynolds number studies of flow across circular cylinders (James et al., 1980; Ruscheweyh, 1982). The pressure distributions therein show characteristics in the supercritical versus the transcritical flow regime consistent with observations from this study at the smooth versus the rough surface. The consistent characteristics are (i) larger absolute suction c_p-values in the crest region, (ii) lower absolute suction c_p-values in the base pressure region, and (iii) a smaller base pressure region, in the supercritical regime or at the smooth surface compared to the transcritical regime or at the rough surface.

Conclusion

It is concluded that in atmospheric-boundary-layer wind tunnel studies at reduced-scale models of low-pressure biogas tanks with hemisphere or (quarter-) calotte roof:

- a supercritical flow regime with associated surface pressure distribution is achieved due to the relatively high turbulence intensity in such type of wind tunnel (typically $20\% < I_U < 40\%$ in the height level of the model),
- a transcritical flow regime with associated surface pressure distribution can be achieved by a rough roof surface.

Hence, the pressure data obtained on the curved roof surface of the model biogas tank without sharp edges (hemisphere roof) and of that without pronounced sharp edges (quarter-

GALA e.V., Karlsruhe, Germany, ISBN 978-3-9816764-9-5

calotte roof) can be reliably transferred to full-scale situations with supercritical or transcritical flow regime when complying with the approach flow turbulence intensity level or the surface roughness, respectively.

References

Achenbach, E., 1972: "Experiments on the flow past spheres at very high Reynolds numbers", J. Fluid Mech., Vol. 54, No. 3, pp.565-575

Bergh, H., Tijdeman, H., 1965: "Theoretical and experimental results for the dynamic response of pressure measuring systems". National Lucht- en Ruimtevaartlaboratorium (NL), report number: NLR-TR F.238, pp.51

Cheng, C.M., Fu, C.L., 2009: "Characteristic of wind loads on a hemispherical dome in smooth flow and turbulent boundary layer flow", J. Wind Eng. Ind. Aerodyn., Vol. 98, pp.328-344

Frank, C., Ruck, B., 2005: "Double-arranged mound-mounted shelterbelts: Influence of porosity on wind reduction between the shelters", Environ. Fluid Mech., Vol. 5, pp.267-292

Gromke, C., Ruck, B., 2008: "Aerodynamic modelling of trees for small-scale wind tunnel studies", Forestry, Vol. 81, pp.243-258

Ikhwan, M., Ruck, B., 2006: "Flow and pressure field characteristics around pyramidal buildings", J. Wind Eng. Ind. Aerodyn., Vol. 94, pp.745-765

James, W.D., Paris, S.W., Malcolm, G.N., 1980: "Study of viscous crossflow effects on circular cylinders at high Reynolds numbers", AIAA J., Vol. 18, pp. 1066-1072

Lippert, O., 2023: "Untersuchungen zur Winddruckverteilung auf Abdeckungen von Niederdruckspeichern für Biogas", Karlsruhe Institute of Technology KIT, Institute for Hydromechanics, Laboratory of Building and Environmental Aerodynamics, BSc thesis pp. 77

Maher, F.J., 1966: "Wind loads in dome-cylinder and dome-cone shapes", J. Struct. Div., Vol. 92, pp.79-96

Maher, F.J., 1965: "Wind loads on basic dome shapes", J. Struct. Div., Vol. 91, pp.219-228

Ruscheweyh, H., 1982: "Dynamische Windwirkung an Bauwerken - Band 1: Grundlagen", pp.96

Savory, E., Toy, N., 1986: "Hemisphere and hemisphere-cylinders in turbulent boundary layers", J. Wind Eng. Ind. Aerodyn., Vol. 23, pp.345-364

Taylor, T.J., 1992: "Wind pressures on a hemispherical dome", J. Wind Eng. Ind. Aerodyn., Vol. 40, pp.199-213

Toy, N., Moss, W.D., Savory, E., 1983: "Wind tunnel studies on a dome in turbulent boundary layers", J. Wind Eng. Ind. Aerodyn., Vol. 11, pp.201-212

GALA e.V., Karlsruhe, Germany, ISBN 978-3-9816764-9-5